HIPPOCAMPUS 13:700–714 (2003)

Dynamically Detuned Oscillations Account for the Coupled Rate and Temporal Code of Place Cell Firing

Máté Lengyel,[1*] Zoltán Szatmáry,[1] and Péter Érdi[1,2]

[1]*Department of Biophysics, KFKI Research Institute for Particle and Nuclear Physics, Hungarian Academy of Sciences, Budapest, Hungary*
[2]*Center for Complex Systems Studies, Kalamazoo College, Kalamazoo, Michigan*

ABSTRACT: Firing of place cells in the exploring rat conveys doubly coded spatial information: both the rate of spikes and their timing relative to the phase of the ongoing field theta oscillation are correlated with the location of the animal. Specifically, the firing rate of a place cell waxes and wanes, while the timing of spikes precesses monotonically as the animal traverses the portion of the environment preferred by the cell. We propose a mechanism for the generation of this firing pattern that can be applied for place cells in all three hippocampal subfields and that encodes spatial information in the output of the cell without relying on topographical connections or topographical input. A single pyramidal cell was modeled so that the cell received rhythmic inhibition in phase with theta field potential oscillation on the soma and was excited on the dendrite with input depending on the speed of the rat. The dendrite sustained an intrinsic membrane potential oscillation, frequency modulated by its input. Firing probability of the cell was determined jointly by somatic and dendritic oscillations. Results were obtained on different levels of abstraction: a purely analytical derivation was arrived at, corroborated by numerical simulations of rate neurons, and an extension of these simulations to spiking neurons was also performed. Realistic patterns of rate and temporal coding emerged and were found to be inseparable. These results may have implications on the robustness of information coding in place cell firing and on the ways information is processed in structures downstream to the hippocampus. © **2003 Wiley-Liss, Inc.**

KEY WORDS: membrane potential oscillation; place field; theta phase precession; hippocampus; model

INTRODUCTION

The debate on whether hippocampal pyramidal cells signal nonspatial as well as spatial information has still not been settled (O'Keefe and Nadel, 1978; Eichenbaum, 1996, 2000; Nadel and Eichenbaum, 1999; O'Keefe, 1999), but that their firing bears considerable spatial correlates is undoubted. However, the ways these spatial correlates are encoded appear to be more elaborate than previously thought as a growing body of experimental data is being collected on the firing characteristics of place cells. Place units, later identified as putative pyramidal cells (Fox and Ranck, 1975) and granule cells (Jung and McNaughton, 1993), were first described in the rat hippocampus as extracellular units signaling whether the animal was inside or outside a well-defined portion (the place field of the unit) of the testing platform (O'Keefe and Dostrovsky, 1971). Mapping spike frequencies to respective locations of the animal during exploration demonstrated that firing of place cells conveys more than binary spatial information (Skaggs et al., 1993): they show centrally peaked graded firing profiles as functions of position both in one-dimensional (O'Keefe, 1976; McNaughton et al., 1983; O'Keefe and Recce, 1993; Skaggs et al., 1996) and two-dimensional (Muller et al., 1987; Gothard et al., 1996), or even in three-dimensional (Knierim et al., 2000; Knierim and McNaughton, 2001), environments. In addition to this finely tuned rate code, the activity of place cells exhibits temporal coding, provided by the phase precession effect, with spikes of a place cell appearing at progressively earlier phases of subsequent cycles of the ongoing field theta oscillation as the animal traverses the place field of the cell (O'Keefe and Recce, 1993; Skaggs et al., 1996). Recently, this phase coding has also been shown to be concurrent with rate coding in virtually any case when field theta was present, and not only during spatial navigation (Harris et al., 2002).

The importance of understanding the generating mechanism of rate and phase-coded place cell firing lies in that both components were shown to have biological significance. In accord with the cognitive map function of the hippocampus (O'Keefe and Nadel, 1978; Muller et al., 1996; Redish, 1999), ensemble activity of place cells was found to be a good predictor of the animal's position in an environment (Wilson and McNaughton, 1993; Fenton and Muller, 1998; Zhang et al., 1998; Redish et al., 2000). This prediction could be improved if

Grant sponsor: Hungarian Scientific Research Fund (OTKA); Grant number: T-025500; Grant number: T-038140; Grant number: AKP-2001-110.
*Correspondence to: Máté Lengyel, Department of Biophysics, KFKI Research Institute for Particle and Nuclear Physics, Hungarian Academy of Sciences, 29-33 Konkoly-Thege M. út, Budapest H-1121, Hungary.
E-mail: lmate@rmki.kfki.hu
Accepted for publication 22 August 2002
DOI 10.1002/hipo.10116

the amplitude modulation of place cell firing frequency by the phase of field theta oscillation was considered (Brown et al., 1998), and it became further refined if a priori knowledge about the position-dependent phase precession of spikes was also incorporated to the position reconstruction process (Jensen and Lisman, 2000). Significance of place reconstruction from place cell activity is supported by that performance on spatial tasks was found to depend on an intact hippocampal place representation (Mizumori et al., 1989; Bures et al., 1997; Lenck-Santini et al., 2001; Brun et al., 2002). Furthermore, choice accuracy was impaired in a working memory task on a radial maze when phase coding was unavailable due to the suppression of field theta, in spite of the preserved rate code in CA1, the main output region of hippocampus proper (Mizumori et al., 1989). This can be explained if downstream areas decoding hippocampal output rely on the phase code of place cell firing (Burgess et al., 1994; Jensen, 2001). Finally, selectivity and stability of place fields, as well as performance in tasks requiring spatial learning, have been found to depend on hippocampal long-term potentiation (LTP) (Shapiro, 2001; but see Holscher, 1999). LTP (Bliss and Lømo, 1973) and long-term depression (LTD) (Lynch et al., 1977), originally described at the level of populations of neurons as a process determined by firing rates, was shown to be sensitive at the single-cell level to the precise timing of pre- and postsynaptic spikes (Paulsen and Sejnowski, 2000; Bi and Poo, 2001). Phase precession of place cells was found to provide ideal conditions for this type of spike timing-dependent plasticity and thus, by accounting for the experience-dependent expansion and shift of place fields (Mehta et al., 1997, 2000), it is generally believed to play a central role in the emergence of place-specific firing in the hippocampus (O'Keefe and Recce, 1993; Skaggs et al., 1996).

The source of this characteristic and doubly coded firing pattern of place cells has been the target of several modeling efforts (O'Keefe and Recce, 1993; Jensen and Lisman, 1996; Tsodyks et al., 1996; Wallenstein and Hasselmo, 1997; Kamondi et al., 1998; Bose et al., 2000; Booth and Bose, 2001; Bose and Recce, 2001) and a few experimental studies applying artificial input to identified pyramidal cells (Kamondi et al., 1998; Magee, 2001). Most of these works made specific assumptions on the anatomical architecture of the modeled area (Jensen and Lisman, 1996; Tsodyks et al., 1996; Wallenstein and Hasselmo, 1997; Bose et al., 2000; Booth and Bose, 2001; Bose and Recce, 2001). Although hippocampal subfields are known to differ significantly in anatomical layout (Lopes da Silva et al., 1990), rate and phase-coded place-specific firing was found in all three subfields (Barnes et al., 1990; O'Keefe and Recce, 1993; Skaggs et al., 1996), CA1, CA3, and the dentate gyrus (DG), and in some cases place fields persisted in downstream areas (CA3 and CA1) even if place-specific input from upstream areas (DG and CA3, respectively) was not available (McNaughton et al., 1989; Mizumori et al., 1989; Brun et al., 2002). Another assumption that is frequently made is that cortical input arriving from the entorhinal cortex (EC) at the hippocampus already contains highly place-specific (topographical) information (Jensen and Lisman, 1996; Wallenstein and Hasselmo, 1997; Booth and Bose, 2001). Although this assumption cannot be rejected, because weakly tuned place cell activity was found in EC (Quirk et al., 1992), we limited our model to the use of minimal spatial information to highlight its ability to generate information on the position of the animal, instead of simply transmitting its input to the output.

Our goal was to construct a model that accounts for the two main characteristics of place cell firing that had not been covered consistently by any previous theories: (1) rate and phase of place cell discharges depend primarily on the position of the animal instead of time spent in the place field, showing a better correlation with the former than with the latter (O'Keefe and Recce, 1993); and (2) firing rate tuning curve of place cells is unimodal with a maximum at the center of the place field, while phase precession curve is decreasing monotonically as the animal traverses the place field (O'Keefe and Recce, 1993; Skaggs et al., 1996). In the present work, we propose a mechanism based on two dynamically detuned oscillators, sharing some theoretical concepts of phase precession first hinted at by O'Keefe and Recce (1993). We show that beyond generating the two salient properties, it also reproduces some finer details of the firing pattern of place cells. First, we derive analytically how the double neural code can emerge from this mechanism. Second, by means of numerical simulations of a rate neuron model, we demonstrate that this derivation is applicable for place cells. Third, by adopting a biologically more plausible spiking neuron model, further firing characteristics of place cells are reproduced. Finally, predictions of the model are given explicitly and are compared with experimental data, where possible, accompanied by an extensive comparison with related models, and possible implications of the inseparable double code of place cell firing on neural coding in the hippocampus and decoding in its efferent structures are discussed.

MATERIALS AND METHODS

Biological Background and Outline of the Model

Throughout our investigations, we modeled the behavior of a single place cell at three different levels of abstraction, where each model described the same two compartmental neuron, proceeding from simple but easily tractable to progressively more complicated but biologically more plausible systems. In all cases, there were four key components to the model:

1. During exploratory behavior, theta field potential oscillation (4–10-Hz frequency and 1–2-mV amplitude) can be recorded from EEG electrodes located in the hippocampus of rats (Green and Arduini, 1954; Vanderwolf, 1969). Field theta oscillation is accompanied by synchronized subthreshold membrane potential-oscillations in the somata of individual pyramidal cells (Artemenko, 1972; Leung and Yim, 1986; Kamondi et al., 1998). This effect is mediated by subcortical disinhibition; i.e., interneurons of the hippocampus are rhythmically inhibited by septal GABAergic afferents (Freund and Antal, 1988; Tóth et al., 1997); alternatively, it is generated within the interneuron network itself (Bland and Colom, 1993; Chapman and Lacaille, 1999a,b; Fischer et al.,

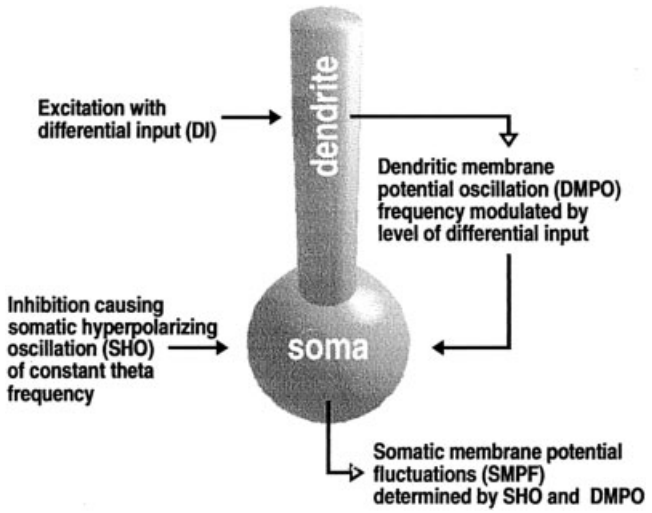

FIGURE 1. Components of the two compartmental model, where the somatic membrane potential fluctuation (SMPF) is influenced by two dynamically detuned oscillations: the rhythmic somatic hyperpolarizing oscillation (SHO) and dendritic membrane potential oscillation (DMPO), the latter being frequency modulated by a velocity-dependent differential input (DI). Firing probability is determined by SMPF.

1999; Orbán et al., 2001), and in either case may be amplified due to resonating properties of the pyramidal cell membrane (Nuñez et al., 1987; Leung and Yim, 1991; Garcia-Munoz et al., 1993; Kiss et al., 2001). This rhythmic somatic hyperpolarizing oscillation (SHO) was incorporated into our modeled pyramidal cell (Fig. 1).

2. Cortical input reaches the hippocampus solely through the entorhinal cortex-perforant path route (Ramón y Cajal, 1893; Lorente de Nó, 1934; Burwell and Amaral, 1998). This input is known to be multimodal and highly preprocessed: place fields—and navigational ability—were indeed found not to depend exclusively on any single modality, or even on individual clues (Maaswinkel and Whishaw, 1999; Poucet et al., 2000; Save et al., 2000). Neurons at different levels of the central nervous system (Derrington and Lennie, 1984; Rauschecker and Harris, 1989; Ingham et al., 2001), and specifically in sensory areas of the cortex belonging to the visual (Livingstone, 1998), auditory (Nelken and Versnel, 2000; Firzlaff and Schuller, 2001), or somatosensory modality (Tremblay et al., 1996; Shoykhet et al., 2000), were shown to be sensitive to the velocity of changes in sensory input. Simultaneous and consistent changes in the input coming from several modalities can most easily be elicited by the motion of the animal. Thus, it is not implausible to assume that hippocampal principal cells receive velocity-dependent input (Bose et al., 2000; Bose and Recce, 2001). Based on these data, velocity-dependent differential input (DI) was assumed to impinge on the dendrite of the modeled neuron (Fig. 1).

3. During REM sleep, when hippocampal field theta is observable (Winson, 1972), the dendritic membrane potential of pyramidal cells was found to oscillate with theta frequency in antiphase with the somatic membrane potential oscillation (Kamondi et al., 1998). Dendrites were also shown to be capable of sustaining intrinsic Ca^{2+}-dependent membrane potential oscillations (DMPOs) with higher frequencies responding to higher levels of depolarization in vivo (Leung and Yim, 1991; Ylinen et al., 1995; Kamondi et al., 1998). Therefore, dendritic membrane potential in our model neuron fluctuated regularly and was frequency modulated by the level of differential input (Fig. 1), thus becoming dynamically detuned from SHO.

4. A widely accepted role of the somata of neurons is to integrate inputs arriving from different sources to the cell. More specifically, it is common to assume that the firing frequency of a typical cortical neuron is close to linear in the summed input current entering the soma, above a threshold (Settanni and Treves, 2000). It was also recognized in earlier works that summing two oscillations with slightly different frequencies could explain the unique firing pattern of place cells (O'Keefe and Recce, 1993). Having identified the two oscillators as the DMPO and SHO, the soma of our model neuron was the integrator of the two oscillations and thus determined firing probability of the cell (Fig. 1).

Equations for the analytical calculations and the rate model, as well as all precise definitions are given in respective subsections of the Appendix. All computations were done with Octave (version 2.0.13) on a Pentium 200-MMX-based PC with a Linux (kernel version 2.0.32) operating system.

Analytical Calculations

First, a mathematical framework was set up in order to track the emergence of phase precession in our model system. Constant frequency SHO followed field theta oscillation with a fixed phase lag. Differential input (D, Eq. A.1) to a cell was defined to be proportional to the instantaneous velocity of the rat within the place field of the cell, and to be zero elsewhere. This input modulated the frequency of DMPO (f_d, Eq. A.2). While DI was zero, the dendritic compartment maintained an oscillation with the frequency of SHO. Higher velocities increased the frequency of DMPO and thus detuned the two oscillators. These two sinusoid oscillations (Ψ_s and Ψ_d, Eq. A.3), one with fixed and the other with varying frequency linearly combined into SMPF (Ψ_C, Eq. A.4). Firing probability of the cell (F, Eq. A.5) was determined by SMPF through a ramp transfer function (Eq. A.6). Constraints for the above assumptions were that DMPO had to be in antiphase with the SHO at both the entry and the exit points of the place field (initial and terminal conditions, respectively, Eq. A.7).

Rate Model

The rate model was developed as a numerical realization of the analytical system. Note that only equations defining the model (Eqs. A.1–A.7 and A.10), and not derived formulae (Eqs. A.8, A.9, A.11–A.18), were used for computing model variables, as it was one of the purposes of these simulations to numerically demonstrate the validity of analytical calculations. To demonstrate the robustness of the model, the animal was allowed to enter the place field at different times (and thus at different phases of field theta and SHO): time and position were no longer taken as relative to the time and position of the entry to the place field (Eq. A.19). This required only some minor changes in the equations used for ana-

lytical derivations and did not alter the mathematical framework in any sense.

Multiple traversals of the place field (trajectories: $x(t)$ functions, used in Eq. A.1) were simulated. The environment (the space where the motion of the model animal manifested) was one-dimensional with a length of $L = 1$ m, representing any kind of linear, circular, or triangular platform (or portion of a more complex environment) used in related experiments (O'Keefe and Recce, 1993; Skaggs et al., 1996). A Monte Carlo simulation was conducted by taking a sample from the pool of possible trajectories on each run. Sampling was done by randomly changing the speed of the animal (i.e., choosing with a uniform distribution from the $S := \{0, 1.5, 2, 3, 4, 4.5, 5, 10, 20, 50$ cm/s$\}$ set) at the ends of fixed time intervals of $\tau_v = 0.5$ s lengths, and keeping the speed constant within these intervals. Twenty passes were simulated through the same place field.

Firing rate measured in experiments was corresponded to firing probability calculated in this model (F^*, Eq. A.21). However, to obtain phase of firing relative to theta, actual times of firing had to be determined. For this purpose, local maxima of the firing probability function were used (Eq. A.22). Firing phase was calculated as the relative phase of cell firing compared with peaks in field theta (ϕ_{sp}, Eq. A.24). For evaluating multiple passes, positions were divided to $N = 20$ discrete bins of $\delta_X = L/N = 5$ cm length. Mean firing probability was calculated in each bin (F_i^*, Eq. A.28) and averages and standard deviations were calculated of both firing probabilities and firing phases over passes.

Numerical realization also required the value of constants to be fixed. Frequency of field theta and thus of SHO was $f_s = 8$ Hz, relative contributions of SHO and DMPO to SMPF were $A_s = A_d = 1$, ratio of speed and the level of differential input was $k_v = 1$ s/cm, distance of entry and exit points of the place field from the beginning of the track were $x_{in} = 10$ cm, and $x_{out} = 50$ cm, respectively, phase of SHO at the beginning of the simulation was $\phi_{s0} = 0°$. Therefore, to satisfy constraints (Eqs. A.7, A.10) depth of frequency modulation of DMPO by differential input was set to $k_D = 1/40$ Hz, and phase of DMPO at the beginning of the simulation was set to $\phi_{d0} = 180°$. Note, that at this level of abstraction, amplitudes (A_s and A_d) and therefore also levels of oscillations (Ψ_s, Ψ_d, and Ψ_C), were still unitless, just as the level of differential input (D) and, naturally, firing probability. For numerical integration, the forward Euler scheme with a simulation time step $\tau = 1$ ms was used.

Spiking Model

An integrate-and-fire model was used to approach biological interpretability of model variables:

$$\dot{V}_m(t) = I_m(t)/C_m \tag{1}$$

where V_m is transmembrane potential, I_m is the net membrane current, and $C_m = 1\ \mu\text{F/cm}^2$ is the membrane capacitance. Firing was defined to occur whenever V_m exceeded a predefined firing threshold $V_\theta = 10$ mV (Eq. A.29), and its phase was determined as in the rate model (ϕ_{sp}, Eq. A.24). At the beginning of each simulation and after each spike, V_m was reset to the resting membrane potential $V_{rest} = 0$ mV. Net membrane current was defined as proportional to instantaneous firing probability obtained from the rate model:

$$I_m(t) := F^*(t) = R^*\left[\frac{\Psi_s(t) + \Psi_d(t)}{A_s + A_d}\right] \tag{2}$$

where Ψ_s and Ψ_d are the currents caused by SHO and DMPO, respectively (Eq. A.3) with amplitudes $A_s = A_d = 200\ \text{nA/cm}^2$ to allow a maximal 40 Hz instantaneous firing rate. Although experimentally observed values are 90–120 Hz (Skaggs et al., 1996), this high rate is attributable to the occasional complex bursting of pyramidal cells. Since the class of integrate-and-fire models we used in this case is not suitable for generating bursts, all spikes in a burst can be considered as if they were substituted with one single spike. R^* is the ramp-transfer function defined in Equation A.20. All other constants were set as in the rate model.

The spiking model was evaluated by simulating multiple passes through the same place field (each pass having a different $X(t)$ function generated by a Monte Carlo simulation, described at the rate model). Information content of spikes was calculated based on the formula used by Skaggs et al. (1996) to permit further quantitative comparison of simulation results with experimental findings:

$$Information = \sum_{i=1}^{N} T_i \frac{F_i}{F} \log_2 \frac{F_i}{F} \tag{3}$$

where F is the overall firing rate (Eq. A.32) and T_i is the occupance probability of bin i (Eq. A.33).

RESULTS

Analytical Calculations

The purpose of analytical calculations was to quantify the dependence of firing probability and phase on the position of the animal, that is, to determine firing profile and phase precession curve. Knowing that instantaneous phase of an oscillation is the integral of its instantaneous frequency over time, this intentionally simple mathematical system was appropriate for analitically calculating both the maximal normalized firing rate ($F_{\max}$, Eq. A.14), based on the amplitude of the envelope oscillation of SMPF (A_C, Eq. A.12), and the phase of SMPF (ϕ_C, Eq. A.16), based on the phase of SHO (ϕ_s, Eq. A.8) and DMPO (ϕ_d, Eq. A.11). Finally, we also calculated the phase lag of SMPF behind field theta (ϕ, Eq. A.18), which was defined as compliant with experimental measures of phase precession (Skaggs et al., 1996).

These two final formulae and Figure 2 show that the probability and phase of spiking depended explicitly only on position, and not on time, in accordance with the experimental findings of Mizumori et al. (1990) showing that the primary correlate of the firing of a place cell is the position of the animal, and those of O'Keefe and Recce (1993) showing a better correlation between firing phase and position than between firing phase and time. This model

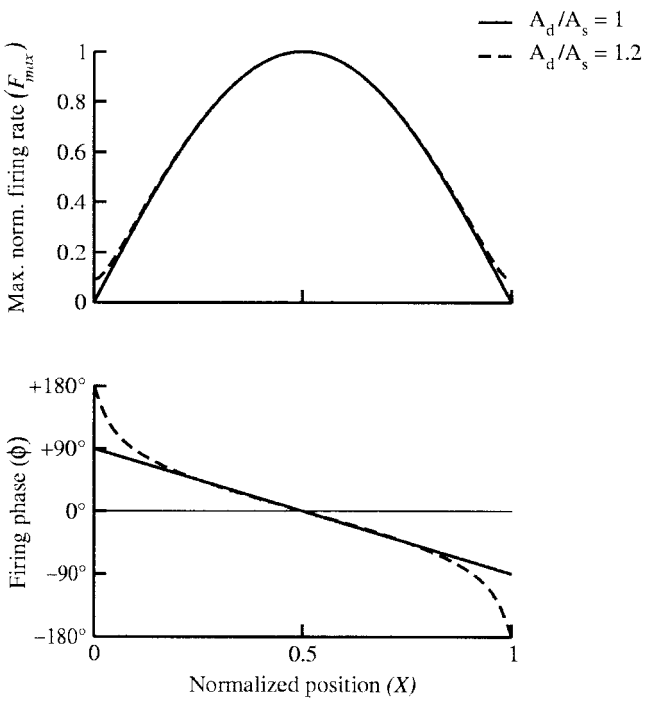

FIGURE 2. Analytical calculations predicted a unimodal firing profile (maximal normalized firing rate (F_{max}), upper plot) and a monotonic phase shift of spikes (firing phase ϕ, lower plot), both depending primarily on position (X). Minor deviation in the ratio of DMPO versus SHO influence on firing ($A_d/A_s = 1.2$, dashed line) had negligible effect on the firing profile but substantially modified the phase precession curve: it was no longer linear and spanned the complete −180°–180° range.

also predicts that if DMPO has a greater influence on firing probability than somatic input ($A_d > A_s$, Eqs. A.3 and A.5), phase precession will be curved instead of purely linear and will span the complete −180°–180° range (Fig. 2, dashed line), as observed in experiments by O'Keefe and Recce (1993) and Skaggs et al. (1996). [Note, however, that the curve predicted by the model is concave-up in the first half of the place field, which is not in agreement with experimental data (Skaggs et al., 1996) fitted with curves concave-down through the whole span of the place field. This mismatch appears to be eliminated by the spiking model, as shown by Fig. 5C.] Moreover, the phase of the first spikes when the rat enters the place field will be the same across cells, as in experiments conducted by Skaggs et al. (1996) and Shen et al. (1997); this phase will consistently be within the 90–180° range after the phase of maximal pyramidal cell activity (Fig. 2), in accordance with measurements of Skaggs et al. (1996). Phase of the last spikes at exit from the place field will be around 90–180° before the population activity peak (as indicated by Fig. 2), but the total shift can be less, as seen in some cases, reported by Skaggs et al. (1996), if frequency modulation of DMPO by differential input is decreased ($k < 1/X_{out}$, cf. Eq. A.10).

Expected information content of the input and output of the modeled neuron was also assessed on the basis of experimentally applied measures (Skaggs et al., 1993, 1996; see also Eq. 3). Average input was defined as a uniform distribution over the place field, a valid assumption within our model framework, if the running speed of the rat does not depend on its position. The output of the model was its firing profile, assuming that the spatial distribution of the rat in space is uniform on average (which again derives from the assumption of location-independent running speed). Spatial information content was shown to be increased from the input to the output, and this increase depended approximately linearly on the relative size of the place field compared with total track length (data not shown). For real place field sizes measured by O'Keefe and Recce (1993), the average expected information content of the input was 2.06 (0.91–3.00) bits/spike, and that of the output was 2.27 (1.12–3.20) bits/spike, for a 11% (7–23%) increase.

Rate Model

The rate model was a numerical realization of the analytical system. Emergence of firing properties of a place cell could be tracked as we iteratively calculated variable values during a traversal of the place field. Figure 3 shows the events involving a single place cell as the animal proceeds in the environment.

Until the rat entered the place field, differential input was defined to be at base level, assumed to be sufficient for the dendritic compartment to maintain an oscillation (DMPO) which was synchronized in antiphase with the rhythmic (theta frequency) hyperpolarizing oscillation of the soma (SHO). The two equal amplitude antiphase oscillations extinguished each other; thus, firing probability was zero in this portion of the environment (Fig. 3A–D, before left arrowhead on time scale). Firing ceased from the moment the rat left the place field (Fig. 3A–D, after right arrowhead on time scale) for the same reasons, that is, the two oscillations became once again synchronized in antiphase here (provided by correctly defining k, the phase shift/distance coefficient, see Eq. A.10), and differential input was switched back to base level.

When position was changing continuously within the place field (Fig. 3A, between arrows) the level of DI stimulating the dendrites was defined to change proportionally to the speed of the animal (Fig. 3B). While frequency of SHO was set to a constant level (Fig. 3C, lower plot), DMPO was allowed to be frequency modulated by DI (Fig. 3C, upper plot). This little jitter caused by frequency modulation was sufficient for DMPO to gain a half-cycle advantage gradually over SHO and consequently escaped the initial antiphase relationship and got exactly into phase with SHO (Fig. 3C, inset). In-phase DMPO and SHO occurred at the middle of the place field. After this point, DMPO continued to gain more advantage over SHO, until a complete cycle advantage was reached (restoring the initial antiphase relationship), where it stopped because the rat left the place field (see above).

SMPF, determined as the linear combination of these two oscillations, changed its frequency and amplitude dynamically (Fig. 3D): the more DMPO was in phase with SHO, the larger the overlap between their peaks became, and consequently the higher the amplitude of SMPF was. As a result, instantaneous firing probability fitted to a centrally peaked firing profile when plotted against position (Fig. 3F). Firing phase, calculated from local maxima of the firing probability function, decreased monotonically during traversal of the place field (Fig. 3E) and turned out to

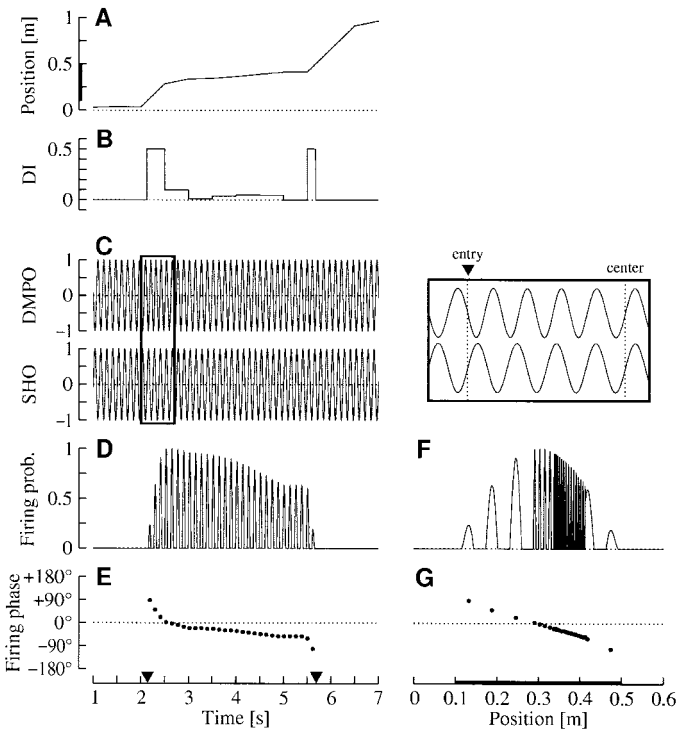

FIGURE 3. Emergence of position dependent firing rate and phase during a single traversal of the place field: the rate model. A: Position of the animal, marked interval: stretch of the place field. B: Level of afferent excitation (proportional to speed) impinging on the place cell, zero corresponding to baseline excitation (see Materials and Methods). C: DMPO with varying frequency (upper plot) and SHO with constant frequency (lower plot), inset shows magnified detail on DMPO (upper trace) gaining a half-cycle advantage over SHO (lower trace) from the time of entering the place field (left vertical dotted line) until reaching its center (right vertical dotted line). D,F: Firing probability (as a linear combination of SHO and DMPO, cut slightly over zero threshold) against time and position. E,G: Phase precession of firing probability peaks relative to peaks in SHO against time and position; bottom: left: time scale for A–E with arrowheads indicating time of entry to and exit from the place field, right: position scale for F–G, marked interval: stretch of the place field. Quantities without explicit indication of unit are unitless at this level of abstraction (see Materials and Methods).

depend just linearly on position (Fig. 3G), as predicted previously by analytical calculations.

Reliability or robustness of the model was assessed by simulating multiple traversals through the place field of the same cell and collecting data to characterize firing probabilities and phases statistically. Following experimental protocols (O'Keefe and Recce, 1993) in which average firing rate profiles are determined after several passes through place fields, and the environment is divided into position bins, we obtained a smooth average firing profile (Fig. 4B, upper plot). However, because of large fluctuations observed during individual passes (Fig. 3F), this smooth average profile was accompanied by an extreme variance of firing probability (Fig. 4B, upper plot). This was in accordance with experimental findings of Fenton and Muller (1998) in which firing of place cells was found to be more variable on individual passes than could be predicted by an inhomogeneous Poisson process depending only on the rat's position and the average firing probability belonging to each position. In our model, this excessive variance emerged, in spite of that maximal firing probability was determined only by the position of the animal (Eq. A.14, Fig. 2), because the actual number of realized spikes during a pass was also determined by a time-dependent term. This term was the phase series of SHO when each location within the place field was visited, which in turn depended on two factors: on the phase of field theta when the rat entered the place field, and more strongly on the actual trajectory of the pass (the

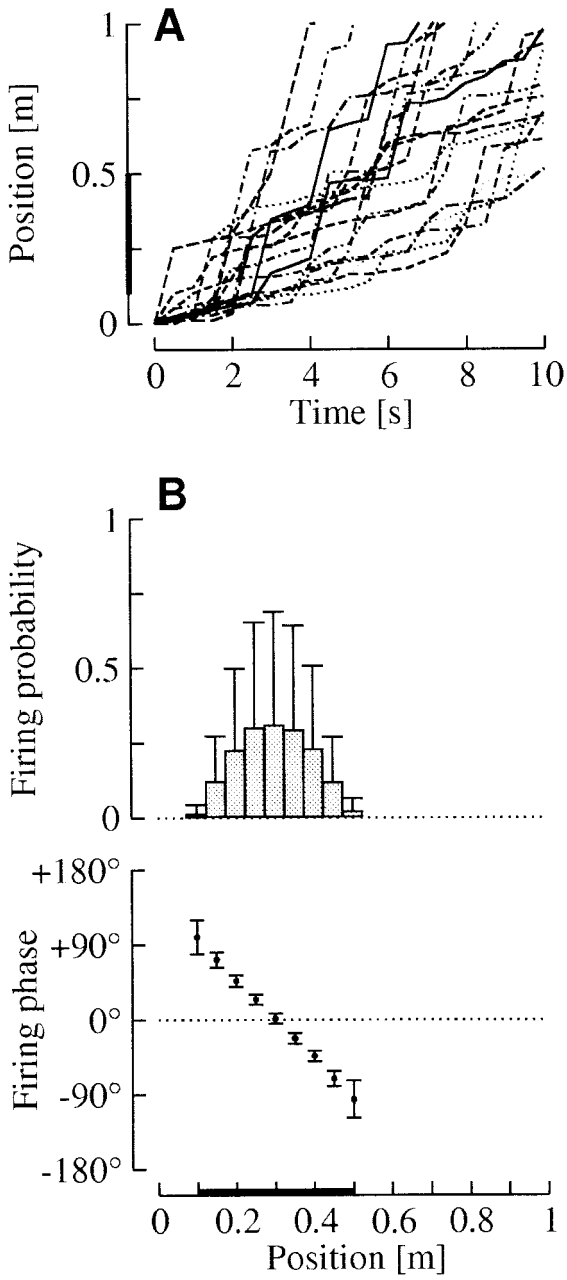

FIGURE 4. Robustness of the model during multiple traversals of the place field: the rate model. A: Trajectories of the animal, marked interval: stretch of the place field, each line represents an individual trajectory. B: Firing probabilities (mean ± SD) (upper plot) and phases (mean ± SD) (lower plot) for 5-cm-long position bins.

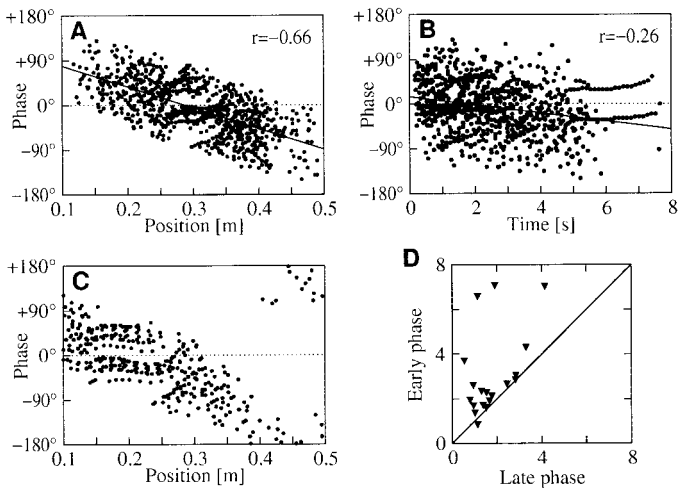

FIGURE 5. Analysis of spike trains generated by the spiking model reveals further matches to experiments. Phases of spikes were better correlated with position (A) than with time spent in the place field (B). Each dot represents one spike. Thick line is fitted by linear regression, with a correlation coefficient *r*. C: Phase precession of spikes extended 360° if dendritic contribution to firing probability was increased ($A_d/A_s = 1.2$). Each dot represents one spike. D: Information content of spikes occurring early within a theta cycle (vertical axis) was significantly more than information conveyed by spikes occurring late (horizontal axis). Each ▼ represents one theta cycle. Correlation coefficients and information contents are unitless.

time elapsed until reaching a given position; see Eqs. A.5, A.13, A.12, A.16, and A.8, in this order).

Phase of firing was less variable and showed a clear linear tendency even after several runs (Fig. 4B, lower plot). Thus the results obtained so far proved to be fairly robust to speed changes and to be independent of actual trajectories, which is a requirement of any reliable and biologically realistic phase precession-firing profile model.

Spiking Model

The spiking model was developed to approach biological reality. The main objective was to generate spike trains based on firing probabilities defined in the rate model. These spike trains could then be further analyzed as in related experiments. Performing these analyses, further place cell properties were reproduced.

A major issue about phase precession concerns its primary correlate, whether it is position or time spent in the place field. This question can only be decided in situations in which the speed of the animal is not constant. Our model clearly showed that both maximal firing rate and firing phase is determined by position (Fig. 2). O'Keefe and Recce (1993), first reporting on phase precession, published quantitative data on the phase precession characteristics of 16 place cells. The correlation coefficients we found (0.66 for position and 0.26 for time in field, Fig. 5A,B) are in good agreement with their results (averages: 0.66 for position and 0.43 for time in field, n = 16). The difference between experiment and model in the correlation with time in field might easily be explained by that the speed of the rat in our model was probably more variable than that of a real animal, chosen to demonstrate the robustness of our results.

Another important experimentally measured property of phase precession is that spikes of a cell tend to span the complete 360° theta cycle (O'Keefe and Recce, 1993; Skaggs et al., 1996; Shen et al., 1997). Although the analytical and rate models predicted firing to occur only in a 180° range (Figs. 2 and 4B), discharges in the spiking model were scattered around the theoretically predicted phase, so that they nearly filled the 360° interval (Fig. 5A). Figure 5C shows that this interval could be further broadened if dendritic contribution to firing probability were greater than somatic ($A_d/A_s > 1$, similar to choosing $p < 0.5$ in a Pinsky-Rinzel model; Pinsky and Rinzel, 1994). In this mode, the model generated a curved crescent-shaped spike cluster that fitted well the nonlinear phase precession patterns observed by Skaggs et al. (1996). Note that the curve of the spike cluster was concave-down through the whole place field, eliminating the mismatch between the prediction of the analytical calculations (Fig. 2) and experimental data (Skaggs et al., 1996). This improvement occurred because the first firings in the spiking model are delayed compared with the analytical model with the time needed to reach the firing threshold by integration, and thus the initial concave-up portion of the firing phase curve shown in Figure 2 is not realized. In the same study by Skaggs et al. (1996), a gradual broadening of spike clusters was also described: phase dispersion of spikes increased from the entry to the exit point of the place field. Our current model cannot account for this phenomenon.

Information content of spikes as a measure of spatial specificity was introduced by Skaggs et al. (1993, 1996) to compare place fields for spikes occurring at different parts of the theta cycle. These investigators found that spikes occurring early in the theta cycle (120°–−60°, with 0° corresponding to maximal pyramidal cell population activity) conveyed significantly more information on the animal's position than those occurring late (−60°–120°) in the theta. (Although this phenomenon was more pronounced in an open field environment, it was still observable in rats running on a triangular track.) Performing the same analysis on our simulated spike trains, our model reproduced these experimental findings (Fig. 5D).

DISCUSSION

We have shown how two compartments of a hippocampal principal cell behaving as two dynamically detuned oscillators can interact to generate the characteristic firing pattern of a place cell (Fig. 3). Position-dependent firing rate and timing were found to emerge in our model without positional information being encoded either in a topographical external input or in topographically ordered recurrent connections (Fig. 1). Matching with experiments using one-dimensional environments, such as linear (O'Keefe and Recce, 1993) or triangular tracks (Skaggs et al., 1996), the model cell had maximal firing rate in the center of its place field with a graded decrease toward the periphery, whereas

the timing of spikes changed monotonically with maximal phase shift at the end of the place field (Fig. 2). Finer details of phase precession, 360° phase span (O'Keefe and Recce, 1993; Skaggs et al., 1996; Shen et al., 1997), and deviation from linearity (Skaggs et al., 1996), were also reproduced, and the parameters controlling these features were determined (Figs. 2 and 5C). These results were demonstrated to be robust to changes in the running speed of the rat (Fig. 4), and, consequently, in line with experimental findings (O'Keefe and Recce, 1993) phase of firing was more correlated to position than to time (Fig. 5A,B).

Two parameters were essential for the model to work that were not explained by biological constraints: (1) the initial phase difference between the dendritic and somatic oscillations at the time of entry to the place field had to be 180°, and (2) the ratio of the frequency of DMPO to the velocity of the animal had to be the reciprocal of place field length (ϕ_{d0} and k, respectively; see Eq. A.10). We outline two candidate mechanisms that can set these values. First, if DMPO is only switched on when DI is above baseline (i.e., when the rat is in the place field of the cell) due to a Hopf bifurcation, which is frequently observable in neuronal membranes (Rinzel and Ermentrout, 1998), a weak background field oscillation can determine its initial phase without interfering with it later, when the system is already oscillating. The experimentally demonstrated antiphasic field oscillation between the perisomatic and dendritic regions of hippocampal pyramidal cells under theta (Kamondi et al., 1998) appears to be suitable for this role. Owing to the same bifurcation, DMPO would be then turned off at exit from the place field thus avoiding sustained firing if the rat ran on a shorter route than that determined by the DMPO frequency/running speed factor (because the factor is not in accord with the size of the place field, or the rat only touched the edge of the place field in a two-dimensional environment). Second, our model predicts that when the rat leaves the place field, DMPO remains at a constant 180° phase lag to SHO. If one or both parameters are not at the values required by our theory, this phase lag will be different, and this difference will be proportional to the mismatches in both parameters. Thus, speculatively, an appropriate learning rule minimizing this phase lag difference as an error signal would optimize simultaneously for both parameters and tune them to their correct values. This hypothetical learning rule would decrease k, which contains a synaptic weight term (k_D, Eq. A.2), if the cell precessed too much, and increase it in the opposite case, resulting in less or more precession, respectively, during the next traversal of the place field. As the input coming from upstream hippocampal areas and the entorhinal cortex to place cells itself is theta modulated (Buzsáki, 2000), the phase lag of DMPO to field theta will determine the postsynaptic voltage in the dendrite that is preferentially paired with presynaptic spikes. LTP and LTD in adult hippocampal slices was recently shown to be inducable by pairing different levels of the postsynaptic membrane potential to presynaptic stimulations at physiological frequencies, when the direction and magnitude of synaptic plasticity depended on the holding potential (Ngezahayo et al., 2000). This may offer a natural mechanism for an appropriate learning rule in our scheme. It is clear, however, that both proposed possibilities need further analysis to assess their robustness and biological plausibility; future versions of the model will incorporate a quantitative description of the dynamics delineated here.

Related Work

Because of the relatively recent discovery of phase precession (O'Keefe and Recce, 1993) compared with the first published observations on place cells (O'Keefe and Dostrovsky, 1971), only a few models, computer simulations, or experiments on in vitro or anesthetized preparations dealt with both the rate and phase code of place cells. Some of these models had been constructed along concepts similar to ours. Two slightly and statically detuned abstract oscillations had been hypothetized earlier as the source of phase precession by O'Keefe and Recce (1993). Two oscillatory inputs of a pyramidal cell explained place cell firing in the work of Kamondi et al. (1998) and Magee (2001). The oscillations were set permanently to be in antiphase and, instead of frequency modulation, the DC component of the dendritic oscillation was modulated by a topographical input. Oscillations along periodic orbits of a system consisting of three or four dynamically coupled neurons gave rise to phase precession in the model of Bose et al. (2000) and Bose and Recce (2001). Gradually increasing the level of feedback inhibition interacting with rhythmic input in the theta range in a pyramidal cell-interneuron pair generated place cell firing, in the work of Booth and Bose (2001). A different class of models, using recurrent networks (attractor networks or chains models), were developed to account for the characteristics of place cell firing by several investigators (Jensen and Lisman, 1996; Tsodyks et al., 1996; Wallenstein and Hasselmo, 1997). In these models, external input excited exclusively (or was biased to) a single cell (or set of cells) at the beginning of each theta cycle and activity then propagated to other cells during the rest of the cycle, as determined by the internal dynamics of the network. Our work differs from all the above-described models in important aspects.

We made no specific assumptions on the anatomical architecture of the area containing our modeled place cell, as long as the necessary inputs (somatic input causing SHO and dendritic differential input causing DMPO) are provided (Fig. 1). A series of reports (Bose et al., 2000; Booth and Bose, 2001; Bose and Recce, 2001) were built on the assumption that pyramidal cells and interneurons were interconnected in a 1:1 fashion, either at the level of single cells or at the level of strictly clustered neurons. However, morphological data on the widely spread dendritic tree and axon arborization of pyramidal cells (Ramón y Cajal, 1893; Lorente de Nó, 1934), as well as of most interneuron types (Freund and Buzsáki, 1996) in the hippocampus, suggest significant convergence and divergence between these cells. Recurrent network models (Jensen and Lisman, 1996; Tsodyks et al., 1996; Wallenstein and Hasselmo, 1997) rely on topographically ordered recurrent connections between place cells, and are thus directly applicable to CA3 only. Note that place cells in CA1 continue to show place fields in the absence of place-specific firing in CA3 (Mizumori et al., 1989) or after isolation of CA1 from CA3 (Brun et al., 2002). Therefore, it is not sufficient to explain this phenomenon in a recurrent network and simply assume that place cells in other regions of the hippocampal formation are driven directly by its out-

put. Our approach allows the model to be applied to any subfield of the hippocampus where place cells were observed: CA1, CA3, and the dentate gyrus (Barnes et al., 1990; O'Keefe and Recce, 1993; Skaggs et al., 1996), despite the significant differences in their anatomical layouts (Lopes da Silva et al., 1990).

Our model neuron produced a ~10% increase of spatial information in its output compared to its input. In some of the alternative models (Jensen and Lisman, 1996; Wallenstein and Hasselmo, 1997; Bose et al., 2000; Bose and Recce, 2001), a Gaussian- or ramp-like firing profile results from the premise that each place cell is only excited at a single location. Thus, in these models, spatial information is either decreased or at best preserved. How much topography is present in the cortical input reaching place cells is unclear; although location dependent activity was found in the entorhinal cortex, this activity was significantly less place-specific than that of hippocampal place cells (Quirk et al., 1992). We believe that as long as strongly location-dependent cortical input to place cells is not demonstrated convincingly in experiments, models should assume as little topography in the cortical input as possible.

Firing rate and phase in our model were better correlated with location than with time (see above), in accord with experimental data (O'Keefe and Recce, 1993). Specifically, the phase of every spike is always correlated better with position than with time, in contrast with recurrent network models (Jensen and Lisman, 1996; Tsodyks et al., 1996; Wallenstein and Hasselmo, 1997) in which phase precession of all spikes, but the first in each theta cycle is time dependent instead of location dependent. However, experimental data should be further analyzed on a finer time scale to reach a conclusion on this point. The recurrent mechanism predicts that the more speed fluctuations occur within a theta cycle the better spikes will be correlated with time instead of position. Our model predicts the opposite: discharges will be more correlated with position in this case. A per-theta cycle analysis of experimental data would reveal the true correlations.

Our model predicted a monotonic phase shift and a unimodal firing rate distribution over locations; i.e., firing rate waxed as the animal approached the center of the place field and waned as the animal left the center and moved towards the periphery, while discharges appeared at consistently earlier phases of subsequent cycles of the theta oscillation during a pass through the place field. Recurrent network models, when tuned to reproduce monotonic phase precession (Jensen and Lisman, 1996; Tsodyks et al., 1996; Wallenstein and Hasselmo, 1997), and coupled oscillator models (Bose et al., 2000; Bose and Recce, 2001) show only a weak, if any, modulation of firing rate by the position of the animal within the place field, resulting in a nearly constant firing rate. Models in which both firing rate and phase are linear or monotonic functions of the same parameter (Kamondi et al., 1998; Booth and Bose, 2001; Magee, 2001) produce a monotonically increasing firing rate if monotonic phase precession is preserved, or a nonmonotonic phase precession if unimodality of the firing profile is to be preserved. Although there is some controversy as to whether phase precession is linear or accelerating, its trend is undoubtedly monotonic (O'Keefe and Recce, 1993; Skaggs et al., 1996). In contrast, most experimental data indicated that firing rate changed in a waxing-waning manner in both one- and two-dimensional environments (McNaughton et al., 1983; O'Keefe and Recce, 1993; Redish et al., 2001), although a recent report by Mehta et al. (2000) showed that firing profiles became asymmetrical with experience: they were clearly Gaussian-like during the first laps on a track but became increasingly skewed on subsequent laps, resulting in an elongated waxing and a short waning phase. Note that although skewness of firing profiles in this study increased, they never became monotonic. Instead, a slowly increasing tail was added at the side of entry to the initially Gaussian-like shapes, also marked by a gradual increase and backward shift of place fields (Mehta et al., 1997). This finding indicates that a symmetrical bell-shaped curve is a better description of the firing profile than any monotonic function at the beginning of an exploration period and that it might still be a good approximation at later times.

Experimental Predictions

Beyond reproducing a range of salient properties and some finer details of place cell firing, our model made predictions that allow experimental testing. The frequency and time code of place cell firing were found to be inseparable because the same mechanism generated both. This is supported by the finding that spike trains of hippocampal pyramidal cells were simultaneously rate and phase coded whenever field theta oscillation was present, i.e., during navigation on a linear track and in an open field, during wheel running, and even during REM sleep (Harris et al., 2002). Consequently, in general, there should not be any situation when either characteristic is present without the other. More specifically, disrupting the generating mechanism should result in the loss of the location specificity of both the firing rate and the firing phases of place cells.

A key component of the model was the SHO (Fig. 1), which was assumed to follow hippocampal theta field potential oscillation with a constant half-period lag (Fig. 3). Under normal conditions, theta is present in the exploring rat (Green and Arduini, 1954; Vanderwolf, 1969; O'Keefe and Recce, 1993). Abolishing it should not only disallow phase precession, but should also result in the loss of location-specific firing of place cells. This prediction was confirmed by the experiments of Mizumori et al. (1989), in which the reversible inactivation of the septum, a main source of hippocampal theta (Petsche et al., 1962), led to the virtual absence of field potential oscillations in the theta band and the disappearance of place fields of CA3c pyramidal cells. However, in the same set of experiments, Mizumori et al. (1989) also found that this treatment did not alter the place-specific firing of CA1 complex-spike units significantly, despite that EEG signals recorded with the same electrodes used for the detection of unit activity clearly lacked the theta component. There are three possible explanations.

First, field potential oscillations are known to reflect synchronized and coherent currents and membrane potential oscillations over large populations of neurons. The theta frequency EEG signal was no longer detectable because septal inactivation caused the loss of synchrony between individual SHOs of principal cells instead of completely abolishing them. Individual SHOs could be maintained by the regular but partly asynchronous firing of the inter-

neuron network (Chapman and Lacaille, 1999a,b). This assumption is supported by the finding that, in the same study (Mizumori et al., 1989), autocorrelation functions of CA1 (but not CA3c) units still showed some degree of theta modulation during the period when field theta was suppressed. This way individual pyramidal cells could still have theta frequency SHOs, and therefore preserve their proper place-tuning curves.

Second, maintenance of individual SHOs can be provided by the theta frequency resonance of pyramidal cell membrane to tonic depolarization (Nuñez et al., 1987; Leung and Yim, 1991; Garcia-Munoz et al., 1993; Kiss et al., 2001). The septohippocampal pathway involves multiple fiber systems (Lopes da Silva et al., 1990), and the necessary depolarization could still be present, even in the absence of the oscillatory component of the septal input.

Both the first and second explanations imply that septal input is necessary for synchronizing spontaneous theta frequency membrane potential oscillations in hippocampal cells, and that this intrahippocampal theta is more robust in CA1 than in CA3. More detailed investigations of theta-generating mechanisms will be necessary to test these predictions. Furthermore, in CA1 even in the absence of field theta, membrane potential oscillations in the theta band should be found in properly tuned individual pyramidal cells, and these cells should show phase precession relative to their somatic oscillations.

Finally, the possibility of alternative ways of generating location-specific firing in place cells, and that different hippocampal subfields might employ different mechanisms, cannot be excluded. In this case, the mechanism of CA1 place cell firing, at least under conditions when theta is not present, remains to be the subject of further studies.

Decoupling of the frequency and phase code of place cells appears to occur naturally when rats are exploring an open platform instead of a circular, triangular, or linear track. Place fields were shown to be robust in environments in which the rat could move freely in two dimensions (Muller et al., 1987; Gothard et al., 1996), while Skaggs et al. (1996) showed that phase precession was much less obvious in such environments than on tracks on which the movement of the rat was confined to a single dimension. The formalism of our model assumes that location within a place field is unambigiously determined by the distance taken from the entry to it. This is valid for one-dimensional environments, provided that different place fields develop for the same region if the rat is allowed to approach it from opposite directions (McNaughton et al., 1983; Markus et al., 1995). If rate and phase of firing depend on the distance traveled within the place field, it leads to the proper frequency and timing of spikes in one-dimensional, but not in two-dimensional, environments in which each location can be approached through trajectories of different lengths and place fields are not direction dependent (Muller et al., 1994). This trajectory dependence is most prominent at the periphery of a place field where the same location can be either at the beginning or at the end of a trajectory and therefore would correspond to the opposite endpoints of a one-dimensional place field. Symmetrically opposing locations within a place field possess similar firing frequency values while, because of the monotonic phase shift of spikes, greatly different firing phases (Fig. 2). Therefore, our model predicts that averaging over multiple trajectories in two-dimensional environments will preserve firing tuning curves but will obscure firing phase-position dependence, as seen by Skaggs et al. (1996). In contrast, our model also predicts that the original phase precession effect can be disclosed by analyzing individual trajectories and plotting spike phases as a function of distance traveled since entry to the place field. In the same experiment (Skaggs et al., 1996), exploration episodes were classified based on the head direction of the animal, and when spikes belonging to different classes were analyzed separately, phase precession similar to which occurs on a linear track could be observed.

Implications for Neural Coding in the Hippocampus and Decoding in Its Efferent Structures

Jointly generated rate and phase code of place cells may have several benefits in terms of neural coding. First, the double code provides structures downstream to the hippocampus with the potential of employing alternative ways of decoding place cell firing. Possible ways of interpreting and using the rate component of this code have been the subject of numerous works (Wilson and McNaughton, 1993; Brown et al., 1998; Zhang et al., 1998); information transfer at the decoding of phase coded spike trains by rhythmically coupled networks has also recently been described (Jensen, 2001).

Second, redundancy in the rate code due to its symmetry is counterbalanced by the uniqueness of the phase code provided by the monotonic phase precession effect, while sensitivity of the phase code to the direction of movement is compensated for by the robust frequency tuning of place cells in two-dimensional environments (see above). These effects will contribute to increasing the accuracy of place reconstruction in areas reading the hippocampal code (Jensen and Lisman, 2000).

Third, activity of several cell types in the hippocampus is theta modulated during related behavior (Skaggs et al., 1993; Csicsvári et al., 1999). Pyramidal cells discharge preferentially at the phase of theta when their membrane potential oscillation is in the most depolarized phase (Ylinen et al., 1995; Kamondi et al., 1998). Because the closer a cell is to its firing threshold, the easier random input discharges it, spikes at this phase may be due to noise without conveying relevant information, as has already been hypothesized earlier by Katona et al. (1999). This is in line with the prediction of our model that in the exploring animal, spikes appearing during the phase of field theta associated with maximal pyramidal cell population activity convey less spatial information than spikes during the rest of the theta cycle (Fig. 5D), as was demonstrated previously in experiments (Skaggs et al., 1993). However, the more rapidly a hippocampal pyramidal cell fires (preferentially in bursts), the more reliably its activity is detected by its postsynaptic partners (Lisman, 1997). Thus, there appears to be a tradeoff between the information content and detectability of place cell firing, one being maximal when the other is minimal during a theta cycle. Decoding mechanisms being sensitive for both the phase and frequency of firing might optimize for these two different aspects of the code.

Fourth, different interneuron populations of the hippocampus synapse on different regions of the dendrite of principal cells, in register with different excitatory afferent fiber systems showing considerable layer specificity (Freund and Buzsáki, 1996). These interneurons discharge at different phases of the field theta (Csicsvári et al., 1999) and, when silent, provide windows of time during which transmission of incoming information is not inhibited in the respective afferents (Katona et al., 1999; Wyble et al., 2000), and when modification of synaptic strengths can take effect (Pavlides et al., 1988; Huerta and Lisman, 1995; Wallenstein and Hasselmo, 1997). Thus, when calculating the effectiveness of the transmission of information and its influence on plasticity, not only should firing rates and relative timing of pre- and postsynaptic neurons be taken into account, but timing of spikes relative to the global oscillation and other neuron populations as well. The double neural code of place cells influences all these aspects, and understanding its mechanism is substantial to our understanding of the hippocampal function.

Acknowledgments

The authors thank G. Orbán for helpful discussions and for critical reading of the manuscript.

REFERENCES

Artemenko DP. 1972. Participation of hippocampal neurons in the generation of theta waves. Neirofiziologiia 4:531–539.

Barnes CA, McNaughton BL, Mizumori SJY, Leonard BW, Lin LH. 1990. Comparison of spatial and temporal characteristics of neuronal activity in sequential stages of hippocampal processing. Prog Brain Res 83:287–300.

Bi G, Poo M. 2001. Synaptic modification by correlated activity: Hebb's postulate revisited. Annu Rev Neurosci 24:139–166.

Bland BH, Colom LV. 1993. Extrinsic and intrinsic properties underlying oscillation and synchrony in limbic cortex. Prog Neurobiol 41:157–208.

Bliss TVP, Lømo T. 1973. Long-lasting potentiation of synaptic transmission in the dentate area of the anaesthetized rabbit following stimulation of the perforant path. J Physiol (Lond) 232:331–356.

Booth V, Bose A. 2001. Neural mechanisms for generating rate and temporal codes in model CA3 pyramidal cells. J Neurophysiol 85:2432–2445.

Bose A, Recce M. 2001. Phase precession and phase-locking of hippocampal pyramidal cells. Hippocampus 11:204–215.

Bose A, Booth V, Recce M. 2000. A temporal mechanism for generating the phase precession of hippocampal place cells. J Comput Neurosci 9:5–30.

Brown EN, Frank LM, Tang D, Quirk MC, Wilson MA. 1998. A statistical paradigm for neural spike train decoding applied to position prediction from ensemble firing patterns of rat hippocampal place cells. J Neurosci 18:7411–7425.

Brun VH, Otnass MK, Molden S, Steffenach HA, Witter MP, Moser MB, Moser EI. 2002. Place cells and place recognition maintained by direct entorhinal-hippocampal circuitry. Science 296:2243–2246.

Bures J, Fenton AA, Kaminsky Y, Zinyuk L. 1997. Place cells and place navigation. Proc Natl Acad Sci U S A 94:343–350.

Burgess N, Recce M, O'Keefe J. 1994. A model of hippocampal function. Neural Netw 7:1065–1081.

Burwell RD, Amaral DG. 1998. Cortical afferents of the perirhinal, postrhinal, and entorhinal cortices of the rat. J Comp Neurol 398:179–205.

Buzsáki G. 2000. Theta oscillations in the hippocampus. Neuron 33:325–340.

Chapman CA, Lacaille JC. 1990a. Cholinergic induction of theta-frequency oscillations in hippocampal inhibitory interneurons and pacing of pyramidal cell firing. J Neurosci 19:8637–8645.

Chapman CA, Lacaille JC. 1999b. Intrinsic theta-frequency membrane potential oscillations in hippocampal CA1 interneurons of stratum lacunosum-moleculare. J Neurophysiol 81:1296–1307.

Csicsvári J, Hirase H, Czurkó A, Mamiya A, Buzsáki G. 1999. Oscillatory coupling of hippocampal pyramidal cells and interneurons in the behaving rat. J Neurosci 19:274–287.

Derrington AM, Lennie P. 1984. Spatial and temporal contrast sensitivities of neurones in lateral geniculate nucleus of macaque. J Physiol (Lond) 357:219–240.

Eichenbaum H. 1996. Is the rodent hippocampus just for "place"? Curr Opin Neurobiol 6:187–195.

Eichenbaum H. 2000. Hippocampus: mapping or memory? Curr Biol 10:R785–R787.

Fenton AA, Muller RU. 1998. Place cell discharge is extremely variable during individual passes of the rat through the firing field. Proc Natl Sci U S A 95:3182–3187.

Firzlaff U, Schuller G. 2001. Cortical representation of acoustic motion in the rufous horseshoe bat, *Rhinolophus rouxi.* Eur J Neurosci 13:1209–1220.

Fischer Y, Gähwiler BH, Thompson SM. 1999. Activation of intrinsic hippocampal theta oscillations by acetylcholine in rat septo-hippocampal cocultures. J Physiol (Lond) 519:405–413.

Fox SE, Ranck JB Jr. 1975. Localization and anatomical identification of theta and complex spike cells in dorsal hippocampal formation of rats. Exp Neurol 49:299–313.

Freund TF, Antal M. 1988. GABA-containing neurons in the septum control inhibitory interneurons in the hippocampus. Nature 336:170–173.

Freund TF, Buzsáki G. 1996. Interneurons of the hippocampus. Hippocampus 6:347–470.

Garcia-Munoz A, Barrio LC, Buno W. 1993. Membrane potential oscillations in CA1 hippocampal pyramidal neurons in vitro: intrinsic rhythms and fluctuations entrained by sinusoidal injected current. Exp Brain Res 97:325–333.

Gothard KM, Skaggs WE, Moore KM, McNaughton BL. 1996. Binding of hippocampal CA1 neural activity to multiple reference frames in a landmark-based navigation task. J Neurosci 16:823–835.

Green J, Arduini A. 1954. Hippocampal electrical activity in arousal. J Neurophysiol 17:533–557.

Harris KD, Henze DA, Hirase H, Leinekugel X, Dragoi G, Czurkó A, Buzsáki G. 2002. Spike train dynamics predicts theta-related phase precession in hippocampal pyramidal cells. Nature 417:738–741.

Holscher C. 1999. Synaptic plasticity and learning and memory: LTP and beyond. J Neurosci Res 58:62–75.

Huerta PT, Lisman JE. 1995. Bidirectional synaptic plasticity induced by a single burst during cholinergic theta oscillations in CA1 in vitro. Neuron 15:1053–1063.

Ingham NJ, Hart HC, McAlpine D. 2001. Spatial receptive fields of inferior colliculus neurons to auditory apparent motion in free field. J Neurophysiol 85:23–33.

Jensen O. 2001. Information transfer between rhythmically coupled networks: reading the hippocampal phase code. Neural Comput 13:2743–2761.

Jensen O, Lisman JE. 1996. Hippocampal CA3 region predicts memory sequences: accounting for the phase precession of place cells. Learn Mem 3:279–287.

Jensen O, Lisman JE. 2000. Position reconstruction from an ensemble of hippocampal place cells: contribution of theta phase coding. J Neurophysiol 83:2602–2609.

Jung MW, McNaughton BL. 1993. Spatial selectivity of unit activity in the hippocampal granular layer. Hippocampus 3:165–182.
Kamondi A, Acsády L, Wang XJ, Buzsáki G. 1998. Theta oscillation in somata and dendrites of hippocampal pyramidal cells in vivo: activity-dependent phase-precession of action potentials. Hippocampus 8:244–261.
Katona I, Acsády L, Freund TF. 1999. Postsynaptic targets of somatostatin-immunoreactive interneurons in the rat hippocampus. Neuroscience 88:37–55.
Kiss T, Orbán G, Lengyel M, Érdi P. 2001. Intrahippocampal gamma and theta rhythm generation in a network model of inhibitory interneurons. Neurocomputing 38/40:713–719.
Knierim JJ, McNaughton BL. 2001. Hippocampal place-cell firing during movement in three-dimensional space. J Neurophysiol 85:105–116.
Knierim JJ, McNaughton BL, Poe GR. 2000. Three dimensional spatial selectivity of hippocampal neurons during space flight. Nat Neurosci 3:209–210.
Lenck-Santini PP, Save E, Poucet B. 2001. Evidence for a relationship between place-cell spatial firing and spatial memory performance. Hippocampus 11:377–390.
Leung LS, Yim CY. 1986. Intracellular records of theta rhythm in hippocampal CA1 cells of the rat. Brain Res 367:323–327.
Leung LS, Yim CY. 1991. Intrinsic membrane potential oscillations in hippocampal neurons in vitro. Brain Res 553:261–274.
Lisman JE. 1997. Burst as a unit of neural information: making unreliable synapses reliable. Trends Neurosci 20:38–43.
Livingstone MS. 1998. Mechanisms of direction selectivity in macaque V1. Neuron 20:509–526.
Lopes da Silva FH, Witter MP, Boeijinga PH, Lohman AH. 1990. Anatomic organization and physiology of the limbic cortex. Physiol Rev 70:453–511.
Lorente de Nó R. 1934. Studies on the structure of the cerebral cortex. II. Continuation on the structure of the ammonic system. J Psychol Neurol 46:113–177.
Lynch GS, Dunwiddie T, Gribkoff V. 1977. Heterosynaptic depression: a postsynaptic correlate of long-term potentiation. Nature 266:737–739.
Maaswinkel H, Whishaw IQ. 1990. Homing with locale, taxon, and dead reckoning strategies by foraging rats: sensory hierarchy in spatial navigation. Behav Brain Res 99:143–152.
Magee JC. 2001. Dendritic mechanisms of phase precession in hippocampal CA1 pyramidal neurons. J Neurophysiol 86:528–532.
Markus EJ, Qin YL, Leonard B, Skaggs WE, McNaughton BL, Barnes CA. 1995. Interactions between location and task affect the spatial and directional firing of hippocampal neurons. J Neurosci 15:7079–7094.
McNaughton BL, Barnes CA, O'Keefe J. 1983. The contributions of position, direction, and velocity to single unit activity in the hippocampus of freely-moving rats. Exp Brain Res 52:41–49.
McNaughton BL, Barnes CA, Meltzer J, Sutherland RJ. 1989. Hippocampal granule cells are necessary for normal spatial learning but not for spatially-selective pyramidal cell discharge. Exp Brain Res 76:485–496.
Mehta MR, Barnes CA, McNaughton BL. 1997. Experience-dependent, asymmetric expansion of hippocampal place fields. Proc Natl Acad Sci U S A 94:8918–8921.
Mehta MR, Quirk MC, Wilson MA. 2000. Experience-dependent asymmetric shape of hippocampal receptive fields. Neuron 25:707–715.
Mizumori SJY, McNaughton BL, Barnes CA, Fox KB. 1989. Preserved spatial coding in hippocampal CA1 pyramidal cells during reversible suppression of CA3c output: evidence for pattern completion in hippocampus. J Neurosci 9:3915–3928.
Mizumori SJY, Barnes CA, McNaughton BL. 1990. Behavioral correlates of theta-on and theta-off cells recorded from hippocampal formation of mature young and aged rats. Exp Brain Res 80:365–373.
Muller RU, Kubie JL, Ranck JB Jr. 1987. Spatial firing patterns of hippocampal complex-spike cells in a fixed environment. J Neurosci 7:1935–1950.
Muller RU, Bostock E, Taube JS, Kubie JL. 1994. On the directional firing properties of hippocampal place cells. J Neurosci 14:7235–7251.
Muller RU, Stead M, Pach J. 1996. The hippocampus as a cognitive graph. J Gen Physiol 107:663–694.
Nadel L, Eichenbaum H. 1999. Introduction to the special issue on place cells. Hippocampus 9:341–345.
Nelken I, Versnel H. 2000. Responses to linear and logarithmic frequency-modulated sweeps in ferret primary auditory cortex. Eur J Neurosci 12:549–562.
Ngezahayo A, Schachner M, Artola A. 2000. Synaptic activity modulates the induction of bidirectional synaptic changes in adult mouse hippocampus. J Neurosci 20:2451–2458.
Nuñez A, Garcia-Austt E, Buno W Jr. 1987. Intracellular theta-rhythm generation in identified hippocampal pyramids. Brain Res 416:289–300.
O'Keefe J. 1976. Place units in the hippocampus of the freely moving rat. Exp Neurol 51:78–109.
O'Keefe J. 1999. Do hippocampal pyramidal cells signal non-spatial as well as spatial information? Hippocampus 9:352–364.
O'Keefe J, Conway DH. 1978. Hippocampal place units in the freely moving rat: why they fire where they fire. Exp Brain Res 31:573–590.
O'Keefe J, Dostrovsky J. 1971. The hippocampus as a spatial map. Preliminary evidence from unit activity in the freely moving rat. Brain Res 34:171–175.
O'Keefe J, Nadel L. 1978. The hippocampus as a cognitive map. Oxford: Clarendon Press.
O'Keefe J, Recce ML. 1993. Phase relationship between hippocampal place units and the EEG theta rhythm. Hippocampus 3:317–330.
Orbán G, Kiss T, Lengyel M, Érdi P. 2001. Hippocampal rhythm generation: gamma-related theta-frequency resonance in CA3 interneurons. Biol Cybern 84:123–132.
Paulsen O, Sejnowski TJ. 2000. Natural patterns of activity and long-term synaptic plasticity. Curr Opin Neurobiol 10:172–179.
Pavlides C, Greenstein YJ, Grudman M, Winson J. 1988. Long-term potentiation in the dentate gyrus is induced preferentially on the positive phase of theta-rhythm. Brain Res 439:383–387.
Petsche H, Stumpf C, Gogolak G. 1962. The significance of the rabbit's septum as a relay station between the mid-brain and the hippocampus. I. The control of hippocampal arousal activity by the septum cells. Electroencephalogr Clin Neurophysiol 14:202–211.
Pinsky PF, Rinzel J. 1994. Intrinsic and network rythmogenesis in a reduced Traub model for CA3 neurons. J Comput Neurosci 1:39–60.
Poucet B, Save E, Lenck-Santini PP. 2000. Sensory and memory properties of hippocampal place cells. Rev Neurosci 11:95–111.
Quirk GJ, Muller RU, Kubie JL, Ranck JB Jr. 1992. The positional firing properties of medial entorhinal neurons: description and comparison with hippocampal place cells. J Neurosci 12:1945–1963.
Ramón y Cajal S. 1893. Estructura del asta de Ammon y fascia dentata. An Soc Esp Hist Nat 22:53–114.
Rauschecker JP, Harris LR. 1989. Auditory and visual neurons in the cat's superior colliculus selective for the direction of apparent motion stimuli. Brain Res 490:56–63.
Redish AD. 1999. Beyond the cognitive map: from place cells to episodic memory. Cambridge, MA: MIT Press.
Redish DA, Rosenzweig ES, Bohanick JD, McNaughton BL, Barnes CA. 2000. Dynamics of hippocampal ensemble activity realignment: time versus space. J Neurosci 20:9298–9309.
Redish DA, Battaglia FP, Chawla MK, Ekstrom AD, Gerrard JL, Lipa P, Rosenzweig ES, Worley PF, Guzowski JF, McNaughton BL, Barnes CA. 2001. Independence of firing correlates of anatomically proximate hippocampal pyramidal cells. J Neurosci 21:1–6.
Rinzel J, Ermentrout B. 1998. Analysis of neural excitability and oscillations. In: Koch C, Segev I, editors. Methods in neuronal modeling. Cambridge, MA: MIT Press. p 251–291.
Save E, Nerad L, Poucet B. 2000. Contribution of multiple sensory information to place field stability in hippocampal place cells. Hippocampus 10:64–76.

Settanni G, Treves A. 2000. Analytical model for the effects of learning on spike count distributions. Neural Comput 12:1773–1787.
Shapiro M. 2001. Plasticity, hippocampal place cells, and cognitive maps. Arch Neurol 58:874–881.
Shen J, Barnes CA, McNaughton BL, Skaggs WE, Weaver KL. 1997. The effect of aging on experience-dependent plasticity of hippocampal place cells. J Neurosci 17:6769–6782.
Shoykhet M, Doherty D, Simons DJ. 2000. Coding of deflection velocity and amplitude by whisker primary afferent neurons: implications for higher level processing. Somatosens Mot Res 17:171–180.
Skaggs WE, McNaughton BL, Gothard KM, Markus EJ. 1993. An information-theoretic approach to deciphering the hippocampal code. In: Hanson SJ, Cowan JD, Giles CL, editors. Advances in neural information processing systems. San Mateo, CA: Morgan Kaufmann. p 1030–1037.
Skaggs WE, McNaughton BL, Wilson MA, Barnes CA. 1996. Theta phase precession in hippocampal neuronal populations and the compression of temporal sequences. Hippocampus 6:149–172.
Tóth K, Freund TF, Miles R. 1997. Disinhibition of rat hippocampal pyramidal cells by GABAergic afferents from the septum. J Physiol (Lond) 500:463–474.
Tremblay F, Ageranioti-Belanger SA, Chapman CE. 1996. Cortical mechanisms underlying tactile discrimination in the monkey. I. Role of primary somatosensory cortex in passive texture discrimination. J Neurophysiol 76:3382–3403.
Tsodyks MV, Skaggs WE, Sejnowski TJ, McNaughton BL. 1996. Population dynamics and theta phase precession of hippocampal place cell firing: a spiking neuron model. Hippocampus 6:271–280.
Vanderwolf CH. 1969. Hippocampal electrical activity and voluntary movement in the rat. Electroencephalogr Clin Neurophysiol 26:407–418.
Wallenstein GV, Hasselmo ME. 1997. GABAergic modulation of hippocampal activity: sequence learning, place field development, and the phase precession effect. J Neurophysiol 78:393–408.
Wilson MA, McNaughton BL. 1993. Dynamics of the hippocampal ensemble code for space. Science 261:1055–1058.
Winson J. 1972. Interspecies differences in the occurrence of theta. Behav Biol 7:479–487.
Wyble BP, Linster C, Hasselmo ME. 2000. Size of CA1-evoked synaptic potentials is related to theta rhythm phase in rat hippocampus. J Neurophysiol 83:2138–2144.
Ylinen A, Soltész I, Bragin A, Penttonen M, Sík A, Buzsáki G. 1995. Intracellular correlates of hippocampal theta rhythm in identified pyramidal cells, granule cells, and basket cells. Hippocampus 5:78–90.
Zhang K, Ginzburg I, McNaughton BL, Sejnowski TJ. 1998. Interpreting neuronal population activity by reconstruction: unified framework with application to hippocampal place cells. J Neurophysiol 79:1017–1044.

APPENDIX

Analytic Calculations

Definitions

Soma receives a (hyperpolarizing) sinusoid input with constant f_s frequency. Let $x(t)$, describing the position of the rat at time t, be relative to the entry point of the place field and t be relative to the time of entry into the place field, thus $x(0) = 0$. Let the point of exit from the place field be x_{out} and the time of exit be t_{out}, thus $x(t_{out}) := x_{out}$. Let then normalized position be $X(t) = x(t)/x_{out}$. Differential input is defined to be

$$D(t) := k_v v(t) \mathcal{H}[X(t)] \mathcal{H}[1 - X(t)] \tag{A.1}$$

where v is the speed of the rat, k_v is the constant depth of modulation of DI by speed, and $\mathcal{H}$ denotes the Heaviside function. Frequency of DMPO is

$$f_d(t) := k_D D(t) + f_s \tag{A.2}$$

where k_D is a synaptic weight constant, expressing the depth of modulation of the frequency of DMPO by the level of DI. Levels of SHO and DMPO are

$$\Psi_s(t) := A_s \cos[\phi_s(t)] \quad \text{and} \quad \Psi_d(t) := A_d \cos[\phi_d(t)] \tag{A.3}$$

where ϕ_s and ϕ_d are phases, and A_s and A_d are amplitudes of SHO and DMPO, respectively.

Level of the composite oscillation (SMPF) is

$$\Psi_C(t) := \Psi_s(t) + \Psi_d(t) \tag{A.4}$$

Let the normalized instantaneous firing rate be

$$F(t) := R\left(\frac{\Psi_C(t)}{A_s + A_d}\right) \tag{A.5}$$

with a ramp-transfer function

$$R(x) := x\mathcal{H}(x) \tag{A.6}$$

Furthermore, we want the following constraints to be satisfied:

$$\phi_d(0) := \phi_{d0} = \pi + \phi_s(0) \quad \text{and} \quad \phi_d(t_{out}) := 3\pi + \phi_s(t_{out}) \tag{A.7}$$

Derivation of location-dependent (and time-independent) firing profile and phase precession

Instantaneous phase of an oscillation is the integral of its instantaneous frequency function over time. Therefore, the phase of SHO is

$$\phi_s(t) = 2\pi \int_0^t f_s \, dt' + \phi_{s0} = 2\pi f_s t + \phi_{s0} \tag{A.8}$$

with $\phi_{s0} = \phi_s(0)$ and, knowing that $v(t) = \dot{x}(t)$, and from Eqs. A.1, A.2, and A.8, phase of DMPO is

$$\begin{aligned}\phi_d(t) &= 2\pi \int_0^t f_d(t') \, dt' + \phi_{d0} = \\ &= 2\pi k \int_0^t v(t') \, dt' + 2\pi \int_0^t f_s \, dt' + \phi_{d0} = \\ &= 2\pi k x(t) + \phi_s(t) - \phi_{s0} + \phi_{d0}\end{aligned} \tag{A.9}$$

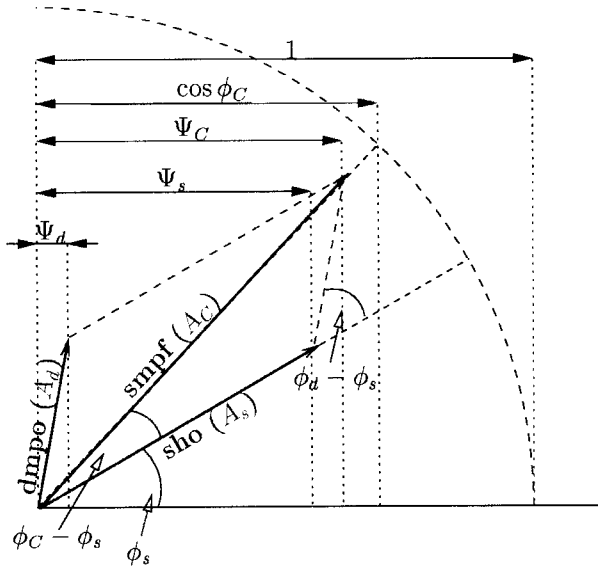

FIGURE 6. Explanatory figure for Equations A.12 and A.16. Vector of the composite oscillation (smpf of A_C length at ϕ_C phase and Ψ_C level) is the sum of the vector of the somatic hyperpolarizing oscillation (sho of A_s length at ϕ_s phase and Ψ_s level) and of the vector of the dendritic oscillation (dmpo of A_d length at ϕ_d phase and Ψ_d level).

where $k = k_v \cdot k_D$. To satisfy constraints of Equation A.7, the values of the constants (from Eqs. A.9 and A.7) have to be

$$\phi_{d0} = \pi + \phi_{s0} \qquad \text{and} \qquad k = \frac{1}{x_{out}} \tag{A.10}$$

Note that this formalism is easily extendable to describe multimodal place fields (O'Keefe and Conway, 1978), and that k only depends on the length of the place field that can be determined without foreseeing the trajectory through the place field; this would not be the case if k depended, for example, on the time of exit.) Thus, the final formula for the phase of DMPO (from Eqs. A.9 and A.10) is

$$\phi_d(t) = 2\pi X(t) + \phi_s(t) + \pi \tag{A.11}$$

With a bit of simple geometry and trigonometry (Fig. 6), it is easy to see that the amplitude of the composite oscillation (SMPF) is

$$A_C(t) = \sqrt{A_s^2 + A_d^2 + 2A_sA_d\cos[\phi_d(t) - \phi_s(t)]} = \\ = \sqrt{A_s^2 + A_d^2 + 2A_sA_d\cos[2\pi X(t) + \pi]} \tag{A.12}$$

and it determines the envelope oscillation, the absolute value the maximal level $\Psi_C(t)$ can reach, given that

$$\Psi_C(t) = A_C(t)\cos\phi_C(t) \tag{A.13}$$

where ϕ_C is the phase of the composite oscillation. It is also provided that maximal normalized firing probability $F_{\max}(t) \geq F(t)$, if defined straightforwardly as

$$F_{\max}(t) = R\left[\frac{A_C(t)}{A_s + A_d}\right] \tag{A.14}$$

Thus, maximal normalized firing probability is shown to depend explicitely only on position and not on time (see also Fig. 2).

It is also apparent that

$$\tan(\phi_C - \phi_s) = \sin(\phi_C - \phi_s)/\cos(\phi_C - \phi_s) = \\ = A_d\sin(\phi_d - \phi_s)/(A_s + A_d\cos[\phi_d - \phi_s]) \tag{A.15}$$

Thus, the phase of SMPF is

$$\phi_C(t) = \arctan2\{A_d\sin[2\pi X(t) + \pi], \\ A_s + A_d\cos[2\pi X(t) + \pi]\} + \phi_s(t) \tag{A.16}$$

Relative phase as used by experimenters measures time difference ratios between discrete events as phases (Eq. A.24). We extended that formula to describe continuous instantaneous phase functions in the following way:

$$\phi(t) = 2\pi f_s\{t - \phi_s^{-1}[\phi_C(t)]\} - \phi_{unit} \tag{A.17}$$

where ϕ_s^{-1} is the inverse function of ϕ_s, and ϕ_{unit} is the phase of theta where maximal pyramidal cell activity is observed. As $\phi_{unit} = 0$ (i.e., maximal unit activity occurred at phase 0 of the perisomatic hyperpolarizing oscillation in our model), on the basis of Equations A.8, A.16, and A.17, the final formula for phase precession is

$$\phi(t) = -\arctan2\{A_d\sin[2\pi X(t) + \pi], \\ A_s + A_d\cos[2\pi X(t) + \pi]\} \tag{A.18}$$

which also depends explicitly only on position, and not on time (see also Fig. 2).

Rate Model

In the rate model, x_{in} and t_{in} were defined so that

$$x_{in} := x(t_{in}) \tag{A.19}$$

Because of numerical constraints, the ramp-transfer function (Eq. A.6) was slightly modified to

$$R^*(x) := x\mathcal{H}(x - 0.0001) \tag{A.20}$$

Thus, instantaneous normalized firing rate changed to

$$F^*(t) := R^*\left(\frac{\Psi_C}{A_s + A_d}\right) \tag{A.21}$$

For calculation of firing phases, the set of spiking times was defined as the set of moments where the normalized firing rate had local maxima:

$$Sp := \{t : \ddot{F}^*(t) = 0\} \cap \{t : \dddot{F}^*(t) < 0\} \tag{A.22}$$

and, similarly, the set of field theta peaks was defined as

$$Tp := \{t : \dot{\Psi}_s(t) = 0\} \cap \{t : \ddot{\Psi}_s(t) < 0\} \tag{A.23}$$

Thus, for any given spiking time $t_{sp} \in Sp$ firing phase was defined to be

$$\phi_{sp} := \frac{t_{sp} - t_p(t_{sp})}{t_f(t_{sp}) - t_p(t_{sp})} \cdot 360° - \phi_{unit} \tag{A.24}$$

where

$$t_p(t_{sp}) := \sup(Tp \cap \{t : t \leq t_{sp}\})$$

and

$$t_f(t_{sp}) := \inf(Tp \cap \{t : t > t_{sp}\})$$

were the times of the preceding and following peaks of the field theta oscillation, respectively, and $\phi_{unit} = 0$, as in the analytical calculations.

Cumulative occupancy of bin i ($1 \leq i \leq N$) was

$$T_i^C := \int_{t=0}^{T_{sim}} \chi_i(t)\, dt \tag{A.25}$$

where T_{sim} is total simulation time (simulation stopped when the animal reached the end of the track: $x(t) = L$) and χ_i indicates whether the animal is within bin i:

$$\chi_i(t) := \begin{cases} 1 & \text{if } (i-1)\delta_X \leq X(t) < i\delta_X \\ 0 & \text{otherwise} \end{cases} \tag{A.26}$$

Cumulative firing rate in bin i was defined similarly:

$$F_i^C := \int_{t=0}^{T_{sim}} F^*(t)\chi_i(t)\, dt \tag{A.27}$$

After each run, we calculated average firing rates:

$$F_i := \frac{F_i^C}{T_i^C} \tag{A.28}$$

Spiking Model

The set of spiking times was redefined to be

$$Sp := \{t : V_m(t) = V_\theta\} \tag{A.29}$$

Therefore, cumulative spike count of bin i was

$$F_i^C := |Sp \cap \{t : \chi_i(t) = 1\}| \tag{A.30}$$

and mean firing rate in bin i became

$$F_i := \frac{F_i^C}{T_i^C} \tag{A.31}$$

and the overall firing rate was

$$F := \frac{\sum_{i=1}^{N} F_i^C}{T_{sim}} \tag{A.32}$$

Occupancy probability of bin i was defined to be

$$T_i := \frac{T_i^C}{T_{sim}} \tag{A.33}$$